Nano Today (2014) 9, 574—589

Available online at www.sciencedirect.com

ScienceDirect

journal homepage: www.elsevier.com/locate/nanotoday

REVIEW

Surgical materials: Current challenges and nano-enabled solutions

Nasim Annabi[a,b,c], Ali Tamayol[a,b], Su Ryon Shin[a,b,c], Amir M. Ghaemmaghami[d], Nicholas A. Peppas[e], Ali Khademhosseini[a,b,c,e,f,g,*]

[a] *Center for Biomaterials Innovation, Department of Medicine, Brigham and Women's Hospital, Harvard Medical School, Boston, MA, USA*
[b] *Harvard-MIT Division of Health Sciences and Technology, Massachusetts Institute of Technology, Cambridge, MA, USA*
[c] *Wyss Institute for Biologically Inspired Engineering, Harvard University, Boston, MA, USA*
[d] *Division of Immunology, School of Life Sciences, Faculty of Medicine and Health Sciences, University of Nottingham, United Kingdom*
[e] *Department of Biomedical Engineering, Department of Chemical Engineering and College of Pharmacy, The University of Texas at Austin, Austin, TX, USA*
[f] *Department of Maxillofacial Biomedical Engineering and Institute of Oral Biology, School of Dentistry, Kyung Hee University, Seoul 130-701, Republic of Korea*
[g] *Department of Physics, King Abdulaziz University, Jeddah 21569, Saudi Arabia*

Received 18 May 2014; received in revised form 28 July 2014; accepted 1 September 2014
Available online 1 November 2014

KEYWORDS
Nano-enabled surgical materials;
Sealants;
Tissue adhesives;
Hemostatic agents;
Antibacterial bioadhesives

Abstract Surgical adhesive biomaterials have emerged as substitutes to sutures and staples in many clinical applications. Nano-enabled materials containing nanoparticles or having a distinct nanotopography have been utilized for generation of a new class of surgical materials with enhanced functionality. In this review, the state of the art in the development of conventional surgical adhesive biomaterials is critically reviewed and their shortcomings are outlined. Recent advancements in generation of nano-enabled surgical materials with their potential future applications are discussed. This review will open new avenues for the innovative development of the next generation of tissue adhesives, hemostats, and sealants with enhanced functionality for various surgical applications.

* Corresponding author at: Center for Biomaterials Innovation, Department of Medicine, Brigham and Women's Hospital, Harvard Medical School, Boston, MA, USA. Tel.: +1 617 768 8395.
E-mail addresses: alik@mit.edu, alik@rics.bwh.harvard.edu (A. Khademhosseini).

http://dx.doi.org/10.1016/j.nantod.2014.09.006
1748-0132/

Introduction

Reconnection of injured tissues after surgery is essential to restore their structure and function. Sutures, wires, and staples are widely used for this purpose, *i.e.*, mostly to hold the tissues in close proximity for fast healing, to resist applied mechanical loads, and to stop body fluid leakages after surgery. Despite their common use in clinic, these methods are not suitable for many procedures, in particular for applications that require preventing body fluid and air leakages. In addition, complete sealing of incisions by sutures generally requires high level of training of surgeons and is particularly challenging for minimally invasive surgeries. In addition, it is challenging to accurately apply sutures and staples in the regions of body that are not easy-to-access. The incision closure procedures using sutures and staples may also induce additional damage in the surrounding tissues in the surgery site. Surgical adhesive biomaterials have emerged as attractive alternatives to stapling and suturing due to their easy application and versatility. These materials can close the incision site more quickly and effectively compared to sutures, which reduces the risk of infection and blood loss by the patient [1,2].

Biomaterials can be used for various surgical operations as tissue adhesives, sealants, and hemostats [3]. Much success has been achieved in hard- and soft-tissue adhesives with the availability of many commercially available bioadhesive systems [4]. Tissue adhesives are surgical materials which can be used to adhere two tissues together, hemostats are mainly used to control bleeding, and sealants act as a barrier to liquid or air [2]. Surgical materials should be biocompatible, easy-to-apply, biodegradable, and inexpensive. They should also possess appropriate mechanical strength and adhesion properties as well as fast curing capability [5]. Commercially available surgical materials are formed from natural or synthetic sources, or a combination of both in the form of composites [6]. Commonly used natural materials for surgical applications include fibrin [7,8], collagen [9], gelatin [10], and polysaccharides [11] and their mixtures. Cyanoacrylates [12,13], various dendrimers [14], polyurethanes (PUs) [15], and poly(ethylene glycol) (PEG) [16] are examples of synthetic surgical materials. Various composite surgical materials have been also formed by using both natural and synthetic polymers such as gelatin-resorcinol-formaldehyde (GRF) [17], albumin/PEG (Progel, Bard Inc.) [18], dextran/(2-hydroxyethyl methacrylate) [19], chitosan/polylysine [20], and PEG/dextran [21].

High cost, limited availability, pro-inflammatory potential, and immunogenicity are some of the limitations associated with naturally derived surgical materials, which limit their use in some surgical procedures. Despite having higher mechanical strength and tissue-bonding properties, synthetic and composite surgical materials have several disadvantages including cytotoxicity, chronic inflammation, low adherence to the wet tissues and, in some cases, long curing time [6].

Recently, extensive research efforts have been made to incorporate nanoscale structures and materials in the design of surgical materials to overcome the aforementioned challenges and provide the next generation of surgical adhesives. For example, it has been demonstrated that aqueous solution of nanoparticles can be used to introduce strong bonding between the tissues without the need for complex *in situ* polymerization or crosslinking reactions [22]. These particle solutions absorb on the surfaces of tissues and act as a connector between the tissues. Nanoparticle solutions can be also used as hemostatic materials to stop internal bleeding with no requirement for specific preparation or control on polymerization reactions as needed for polymer-based hemostatic agent [23]. In addition, various types of nanomaterials have been incorporated into polymer matrices to introduce new functionalities such as providing antibacterial activity. In addition, nanoparticles loaded into surgical materials can improve their adhesion strength and mechanical properties. In general, the use of nanomaterials in the design of tissue adhesive has eliminated the requirement for complex *in vivo* polymerization or crosslinking reactions and led to the development of easy-to-use tissue adhesives and hemostats with improved functionalities for clinical applications. Nanomaterial-incorporated tissue adhesives can address many limitations of currently available tissue adhesives such as toxicity, extensive swelling, insufficient strength, and complex polymerization process. They have the potential to be used instead of sutures and staples in clinical practice, particularly in invasive surgeries to minimize tissue damage.

More recently, an active area of research has focused on developing surgical tissue adhesive with specific nanotopography to engineer biomimetic structures inspired by nature. Nanotopography is deemed as the specific spatiotemporal coordination and distribution of molecular structures that provides detailed and desirable structures. The employed nanotopography can enhance the adhesion force through the augmentation of contact area and the adhesive van der Waals and capillary forces. Moreover, these nanopatterns can be used for creating mechanical interlocking to increase the required detachment forces [24].

In this work, conventional surgical materials made of natural and synthetic polymers are critically reviewed along with their advantages and limitations for surgical applications. Recent developments in synthesis and characterization of nanomaterial incorporated surgical materials with hemostatic and antibacterial properties are discussed. In addition, emerging technologies for generating micro- and nanoscale topography in tissue adhesives to improve their adhesion strength are highlighted.

Conventional surgical materials

Wound closure is a key step in the success of various surgical procedures. Each procedure carries specific risk factors, which should be addressed by utilization of functional bioadhesive that meet these criteria. For example, during vascular anastomosis preoperative bleeding from the surgery site and blood coagulation are among the key risk factors [25]. Thus, the employed tissue adhesives should be hemostatic, while possess sufficient mechanical properties to hold the tissue together. Ease of application and the minimal need for utilization of external devices during the crosslinking process are also important for closing internal surgery lacerations during operation. However, for treating traumatic injuries, the wound closure procedure

should be quick and minimally invasive [26]. The adhesion strength of the bioadhesive should be high enough to prevent tissue detachment after treatment. In addition, ideally the mechanical properties of the bioadhesive materials should mimic the surrounding tissue [27]. The employed tissue adhesive should also form an effective barrier against external risk factors including bacteria and other pathogens. In the following sections we will discuss various types of existing tissue adhesives.

Natural origin surgical materials

Surgical materials based on natural polymers have attracted significant attention due to their biocompatibility and similarity to the tissue microenvironment [28]. These natural surgical materials are obtained from biological sources such as human blood (e.g. fibrin) or formed by chemical crosslinking of various natural polymers including collagen, gelatin, chitosan, alginate, and chondroitin [29].

Fibrin-based surgical materials are one of the most widely used glues in clinical applications. They are made from two main components, fibrinogen and thrombin, with a small quantity of calcium chloride to form surgical materials with dual applications, hemostatic and sealant [30]. Fibrin is polymerized from the fibrinogen and then a white fibrin clot is generated with thrombin and $CaCl_2$. Commercial fibrin-based surgical materials, such as Evicel (Ethicon Inc.), Hemaseel APR (Heamacure Corp.), Tisseel (Baxter Healthcare Corp.), and Crosseal (OMRIX Biopharmaceuticals Ltd.) have been widely used as both hemostatic [31] and sealants [32]. Despite their advantages including biocompatibility, fast curing and biodegradability, poor adhesion properties of fibrin-based glues to the wet tissues and their low mechanical strength under loading make them unsuitable for many surgical procedures [33,34]. Therefore, for some clinical applications, fibrin-based surgical glues should be used along with sutures or staples [35,36]. The use of human-based fibrin glues also carries the risk of disease transmission [34,37].

Collagen-based surgical materials are another type of natural tissue adhesive [38]. The most commonly used collagen-based surgical materials approved for clinical applications are Proceed (Fusion Medical Technologies) [39], a composition of bovine collagen and bovine thrombin, and CoStasis (Cohesion Technologies, Inc.) [40], which is made of human plasma, bovine collagen, and thrombin. Similar to fibrin, collagen-based adhesives have low adhesion and mechanical strength. Gelatin-based bioadhesives such as Floseal™ (Fusion Medical Technologies, Inc.) [41], a combination of bovine gelatin and thrombin, have been also used as hemostatic agents. In another study, photocrosslinkable gelatin sealants with high adhesion strength (more than 100 kPa) and tensile strength (around 2 MPa) were produced to seal vascular, lung, and gastrointestinal defects [10]. Other crosslinking approaches such as chemical crosslinking using aldehyde and microbial transglutaminase (mTG) have also been used to form gelatin-based hemostatic adhesives, which can connect tissues in the absence of sutures [42]. Furthermore, hemostatic materials and tissue adhesives based on a combination of gelatin and poly(L-glutamic acid) have also been developed [34]. Chitosan-based tissue adhesives are another family of commercially available natural surgical materials for clinical applications [43]. Chitosan offers both antibacterial and hemostatic characteristics and has been used in various forms such as powders (e.g. Celox™) or photocrosslinked hydrogels to stop bleeding from the arteries [44].

To improve the mechanical properties and adhesion strength of natural tissue adhesives, composite glues based on a combination of different natural and synthetic components have been developed. One example is the French glue or GRF (GRF glue®), which is a composite of gelatin/resorcinol and formaldehyde [45,46,17]. Due to their ability to provide strong covalent bonding to wet tissues using aldehydes groups, GRF glues have been used in Europe for aortic dissections, liver, urinary tract, and gastrointestinal surgeries. However, the presence of unreacted aldehydes may cause toxicity, which has limited their use in North America [45,46,17]. BioGlue (Cryolife Inc.) is another FDA approved sealants based on a combination of human albumin and glutaraldehyde [47—50]. Although BioGlue has been successfully applied for sealing large blood vessels and aortic dissections, it contains aldehyde that generates safety concerns for clinical applications.

Synthetic and semi-synthetic surgical materials

Various types of synthetic and semi-synthetic materials such as cyanoacrylates, PUs, PEG-based dendrimers, and PEG hydrogels have been used for developing surgical materials for different clinical applications. These surgical materials offer strong adhesive properties and mechanical strength. In addition, their compositions, structures, and physical properties can be tailored for specific applications. Among synthetic tissue adhesives, cyanoacrylates have been widely used for external applications such as closure of skin wounds due to their fast curing, strong adhesion to tissues, and ease of use [51]. The synthetic adhesives based on cyanoacrylate are liquid monomers. These monomers can polymerize rapidly by an anionic mechanism in the presence of water or blood to form a flexible film that bridges the wounds and holds the apposed wound edges together. For example, Dermabond (Ethicon Inc.) is a glue based on 2-octyl cyanoacrylate and has been widely used by surgeons in cosmetic surgery, for closing small lacerations and in skin graft fixation [52]. However, high price and foreign body reaction are some of the limitations associated with the use of Dermabond. Other commercially available cyanoacrylate-based bioadhesives are Trufill n-BCA (Cordis Neurovascular, Inc.), a combination of tantalum powder and n-butyl cyanoacrylate, and Glubran2 (GEM s.r.l.), a modified form of n-butyl-2-cyanoacrylate [51,53]. These products have shown strong adhesive and hemostatic properties for various clinical applications, but they can only be employed for external use due to their potential toxicity and pro-inflammatory characteristic upon contacting non-cutaneous surfaces [54].

Another class of synthetic surgical materials is PEG-based sealants, which are mainly composed of chemically modified linear or branched PEG molecules. Coseal (Cohesion Technologies, Inc.) is a commercially available PEG-based sealant, composed of two four-arm PEG, one with glutaryl-succinimidyl ester terminal groups and the other

one with thiol terminal groups. Upon mixing, covalent bonds between PEG molecules are formed through the reaction between thiol groups and the carbonyl groups of the succinimidylester. Coseal has been widely used for sealing suture lines in vascular grafts [26,54,55].

Duraseal (Covidien Inc.) is another FDA approved PEG-based tissue adhesive, consisting of PEG ester and trilysine amine solutions [56—58]. Duraseal is commonly used by neurosurgeons to stop cerebrospinal fluid leakage following surgeries. A bioresorbable and photocrosslinkable PEG-based sealant, FocalSeal (Genzyme Biosurgery, Inc.), has been developed for thoracic surgery to stop air leaks [59]. FocalSeal has been also used for wound closure and hemostasis in anastomotic bleeding [16,59,60]. PEG-based sealants have several advantages including biocompatibility and relatively high adhesion strength. However, high swelling ratio of PEG-based sealants may cause pressure build up on the surrounding tissues when applied in closed cavities [61]. In addition, the use of UV light and long curing time may limit their clinical applications (e.g. its utilization in hemorrhagic situations).

Recently, PU-based surgical materials have received attention because of their strong adhesion to tissues through the formation of urea bonds [1]. No toxicity has been reported upon utilization of urethane-based bioadhesives for renal surgery, pancreatic occlusion, and orthopedic surgeries. A sprayable PU adhesive, TissuGlu (Cohera Medical Inc.), has been developed for cosmetic procedures as a resorbable and non-toxic tissue adhesive [62]. Prolonged curing times and the possibility of toxic degradation products are potential limitations associated with the utilization of urethane-based materials for clinical applications. Ferreira et al. synthesized biodegradable PU-based adhesives through the reaction between castor oil and isophorone diisocyanate (IPDI) or by reaction of polycaprolactone (PCL) diol with IPDI or hexamethylene diisocyanate (HDI) [63]. Despite significant improvements in the synthesis of biodegradable and biocompatible PU-based surgical materials, safety concerns still exist for their clinical applications. Recently, Lang et al. developed a hydrophobic light-activated tissue adhesive (HLAA) for cardiovascular surgeries [64]. This highly elastic tissue adhesive was formed by photocrosslinking of poly (glycerol sebacate acrylate) (PGSA) in the presence of a photoinitiator and UV light. The result of *in vivo* tests showed no inflammatory reaction after attaching a HLAA coated patch on the rat heart, demonstrating the biocompatibility of the engineered HLAA bioadhesives. In addition, HLAA tissue adhesive was used to close defects in a pig carotid artery without the use of a patch. No bleeding was observed after 24 h of implantation and all animals survived after the procedure. H&E staining of the carotid arteries exhibited an intact endothelium with no thrombus formation, demonstrating the suitability of the HLAA for the repair of vascular defects [64].

One of the limitations of the conventional surgical materials including synthetic glues such as cyanoacrylate or natural bioadhesives like fibrin is their low adhesion in wet environments, which limits their applications for internal use. To address this challenge, scientists have focused on natural models with high adhesion strength to wet surfaces such as marine mussel proteins to mimic their adherence mechanism [65—67].

Mussels (e.g. *Mytilus edulis*) adhere strongly to underwater surfaces by secreting adhesive materials (byssus) from their feet [68]. These adhesive materials contain a bundle of threads with adhesive plaques at the end of the threads to anchor to wet surfaces. It has been shown that this strong adhesion in wet environment is due to the presence of a catechol-containing amino acid L-3,4-dihydroxyphenylalanine (L-DOPA), which enables the crosslinking of mussel adhesive proteins through oxidation of catechol hydroxyl groups to DOPA-quinone [69,70]. The adhesion mechanism of mussels has been mimicked by many research groups to develop tissue adhesives with the ability to adhere to wet surfaces [71,72].

Several researchers initially focused on extraction and purification of adhesive proteins from mussels [73] or synthesis of recombinant mussel proteins [74]. The extracted adhesive proteins were crosslinked to enhance adhesion strength and mechanical properties of the bioadhesives for various clinical applications [75]. However, the use of complicated extraction processes and low yield (1 gr adhesive protein from 10,000 mussels) have limited the production of mussel-derived adhesive proteins [76,77]. To overcome these limitations, researchers synthesized DOPA-containing polypeptides [71] or DOPA functionalized polymers [72]. For example, DOPA-functionalized PEG tissue adhesives were synthesized by using different oxidation agents such as horseradish peroxide, mushroom tyrosinase hydrogen peroxide, and sodium periodate [72].

In another study, surgical meshes coated by DOPA-functionalized PEG and PCL were produced to eliminate the need for mechanical fixation of the mesh for surgical repair of soft tissues [78]. More recently, an injectable and biodegradable citrate-enabled mussel-inspired bioadhesive (iCMBA) was produced using citric acid, dopamine/L-DOPA, and PEG [79]. This synthesized tissue adhesive showed 2.5—10 times higher adhesion strength compared to commercial fibrin glues. *In vivo* studies demonstrated that iCMBA adhesive could rapidly stop bleeding and close open wounds, in the absence of stitches or staples, on the dorsum of a rat model [79]. Mussel-inspired tissue adhesives have shown several advantages for clinical applications such as strong adhesion to the wet tissues, biocompatibility, and biodegradability. Recently, this group of tissue adhesives have been used for various applications including fixation of prosthetic meshes [6], extrahepatic islet transplantation [80], bioadhesives for small intestinal submucosa [81], and injectable sealants for fetal membrane repair [82,83].

Overall, conventional surgical materials have shown to possess significant potential in many clinical applications. However, strong adhesion to wet tissues, biocompatibility, biodegradability, affordable cost, and ease of use are some of the requirements to be addressed. Various research groups have focused on engineering multifunctional surgical materials by merging nanotechnology and advanced biomaterials. For example, one research area has focused on developing nanomaterial-incorporated surgical materials with hemostatic or antibacterial properties. Recently, biomimetic nanostructured tissue adhesives with improved adhesion strength have been also developed. Recent developments in engineering of nano-enabled surgical materials for various clinical applications are highlighted in the following sections.

Nanoparticle incorporated surgical materials

Conventional polymeric tissue adhesives usually require complex *in vivo* control of polymerization or crosslinking reactions. They may also suffer from being toxic, weak, or ineffective within the wet conditions. Nanoscience and nanotechnology play an important role in improving the properties and function of tissue adhesives for clinical applications. For example, nanotechnology enables the use of nanoparticle solutions as adhesives and hemostatic materials to strongly bind biological tissues together and stop internal bleeding without the need of using complex *in situ* polymerization techniques. It has been shown that surface chemistry modification of these nanoparticles can enhance particle adsorption to the tissues and form strong bonding between them [22,23]. In addition, tissue adhesives with antibacterial capabilities can be formed through the incorporation of antimicrobial nanoparticles or hemostatic bioadhesives can be engineered by encapsulation of active nanoparticles in the adhesives [84]. Novel bioadhesives have been also developed for controlled drug-delivery [4,85,86]. In this section, recent advances on the application of nanotechnology in designing multifunctional surgical materials are reviewed. In particular, the use of nanoparticles for engineering antibacterial and hemostatic bioadhesives is discussed. Table 1 summarizes some examples of traditional and nano-enabled adhesive materials with their formulation, adhesion strength, and functionalities.

Hemostatic materials

Hemostatic agents are being increasingly used in various procedures such as hepatic, cardiovascular, spinal, and orthopedic surgeries where hemorrhage control is essential to avoid severe blood loss [87,88]. Suturing is conventionally applied to stop bleeding but it is not effective for controlling rapid bleeding in many procedures. Therefore, hemostats are used during surgeries for fast and effective control of bleeding. These hemostatic agents should be safe, easy-to-apply as well as provide fast blood clotting. Hemostatic materials are classified into two main categories: mechanical and active agents [29]. Mechanical hemostatic agents stop bleeding by generating a mechanical barrier to the blood flow and can be used in forms of sponges, sheets, powders, or particles. Some examples of the commercially available mechanical hemostatic agents include Gelfoam (bovine gelatin, Baxter Inc.), Instat (bovine collagen, Ethicon, Inc.), and Surgicel (oxidized cellulose, Ethicon, Inc.) [61]. Active hemostatic agents contain active biological components such as thrombin, which can participate in blood clotting when applied to the injured sites [29]. Combination of mechanical and active agents has been shown to enhance the hemostatic efficacy [61].

Mineral zeolite materials such as QuikClot (Z-Medica, Wallingford, CT) have had a significant impact on trauma care in clinical applications [89—91]. Mineral zeolite materials absorb liquid in the wound area, thereby increasing the concentration of coagulants to induce hemostasis. The activity of zeolite materials leads to an exothermic reaction in wound bed, which has been addressed by embedding zeolite in a surgical mesh so it can be used as a compress to absorb water less exothermically by using ion exchange technique and prehydration [92,93]. Zeolite materials are inexpensive, stable, easy-to-use, and have shown to have both hemostatic and antibacterial properties [89]. In a clinical study, QuikClot was found to control bleeding in 92% of the 103 documented cases with 100% of the cases performed by first responders [94].

Hemostatic materials can be formed by combining one or two coagulation cascades or hemostatic proteins including thrombin [95], collagen [96], chitosan [97,98], and fibrin [4,99] as well as non-protein materials such as oxidized cellulose [96,100] and PEG [100]. These hemostats have been used in various forms for surgical applications including matrix [96,101], patch [102,103] or liquid [95,99]. The major challenges associated with the clinical use of these hemostatic materials include their high cost and non-effective bleeding control [104].

To address these challenges, micro and nanoparticles have been used as hemostatic agents to control blood loss. For example, in a recent study, cationic hydrogel particles based on N-(3-a-aminopropyl)methacrylamide (APM) were synthesized *via* inverse suspension polymerization and used as hemostatic agents (Figure 1A) [105]. *In vitro* studies confirmed the formation of blood aggregation, which was due to the high swelling ratio of the hydrogel particles (>1000%) as well as their high positive charge. The capability of the engineered particles for rapid hemostasis *in vivo* was also demonstrated by using a tail amputation rat model (Figure 1B and C) and an ovine liver laceration model (Figure 1D and E) [105].

Some research groups have focused on developing hemostatic materials based on functionalized nanoparticles capable of aggregating platelets from blood flow [106—109]. For example, Ravikumar et al. created hemostatic nanomaterials through the surface functionalization of liposomes with 150 nm diameters with three peptides including von Willebrand factor (vWF)-binding peptide (VBP), collagen-binding peptide (CBP) and cyclic-Arg—Gly—Asp (cRGD) peptide [107]. It was shown that liposomes containing VBP and CBP could facilitate platelet-mimetic adhesion and cRGD functionalized liposomes enhanced the aggregation of platelets onto themselves. Therefore, combination of all three peptides provided a dual hemostatic function of aggregation and adhesion [107]. In another study, Bertram et al. engineered functionalized nanoparticles with the capabilities for binding to active platelets to enhance their aggregation rate and consequently stop bleeding [106]. A single emulsion evaporation technique was used to synthesize nanoparticles with the diameter of 170 nm consisted of poly(lactic-co-glycolic acid)-poly-L-lysine (PLGA-PLL) copolymer conjugated with RGD functionalized PEG (Figure 2 A and B). The interaction of engineered nanoparticles with active platelets was assessed *in vitro* by using a platelet adhesion and aggregation assay. These synthetic hemostatic nanoparticles also reduced bleeding after intravenous injection in an injured site in a rat artery by distributing throughout the clot (Figure 2C—E). It was also shown that the nanoparticles were effectively cleared within 24 h after infusion, demonstrating the potential application of the engineered hemostatic nanoparticles for early intervention in trauma [106].

Table 1 Traditional and nano-enabled adhesive materials.

Traditional surgical materials				
Type	**Components**	**Formulation**	**Functionalities**	**Ref.**
Natural biomaterials				
Fibrin-based	Fibrinogen, thrombin, and $CaCl_2$	Fibrin clot formation	Hemostatic, sealant	[7,8,30—37]
Collagen-based	Bovine collagen, thrombin, and plasma	Collagen clot formation	Hemostatic, sealant	[9,38—40]
Gelatin-based	Bovine gelatin, and thrombin	Gelatin clot formation	Hemostatic, sealant	[41]
	Photocrosslinkable gelatin	Photoinitiated polymerization	Sealant	[10]
	Gelatin, and aldehyde, mTG	Chemical crosslinking using aldehyde	Hemostatic, sealant	[42]
	Gelatin, and poly(L-glutamic acid)	Crosslinking bonding using water-soluble carbodiimides	Adhesives, hemostatic	[34]
Polysaccharides	Chitosan powders and photocrosslinkable chitosan	Photoinitiated polymerization	Adhesives, antibacterial, hemostatic	[43,44]
Synthetic biomaterials				
Cyanoacrylate	2-octyl cyanoacrylate, tantalum powder, and n-butyl cyanoacrylate,	Addition polymerization: anionic mechanisam	Adhesives, sealant	[12,13,51—54]
Polyurethanes	Sprayable and biodegradable polyurethane	Addition polymerization	Aesorbable, non-toxic tissue adhesive	[1,15,62—64]
PEG-based	4-arm PEG with glutaryl-succinimidyl ester and thiol terminal groups	Covalent bonds	Sealant	[26,55]
	PEG ester and trilysine amine solutions	Photo or chemical crosslinking	Stop cerebrospinal fluid leakage	[56—58]
	Photocrosslinkable PEG sealant	Photoinitiated polymerization	Stop air leaks, wound closure, and hemostasis	[16,59—61]
Synethic mussel-based	DOPA-PEG, -PCL, and catechol-L-DOPA	Oxidation of catechol groups to DOPA-quinone	Hemostasis, and wound closure	[69—83]
Nano-enabled adhesive materials				
Nanoparticles	Silica nanoparticles	Particle adsorption	Adhesives	[22,23]
	Cellulose nanocrystals	Cellulose complexation	Adhesives	[96,100,110]
	ZnO nanoparticles	Zn complexation	Antibacterial	[119—121,130,131]
	Silver-based nanoparticles	Particle adsorption	Antibacterial, adhesives, wound closing, and hemostatic	[115,123—127,129,132,133]
	Calcium phosphate-based nanoparticles	Metal ion complexation	Antibacterial, adhesives, lower inflammatory response, and tertiary dentin formation	[120,122,123]
Biomimetic nano-structure	Hierarchical mushroom-tipped nanoscale fibrilsto	Combination of van der Waals and capillary forces	Adhesives	[137—142]
	PCL patches covered with microposts	Layer of cyanoacrylate medical glue	Adhesives	[145]
	Silicon nanowires on glass beads	van der Waals forces	Adhesives	[147]

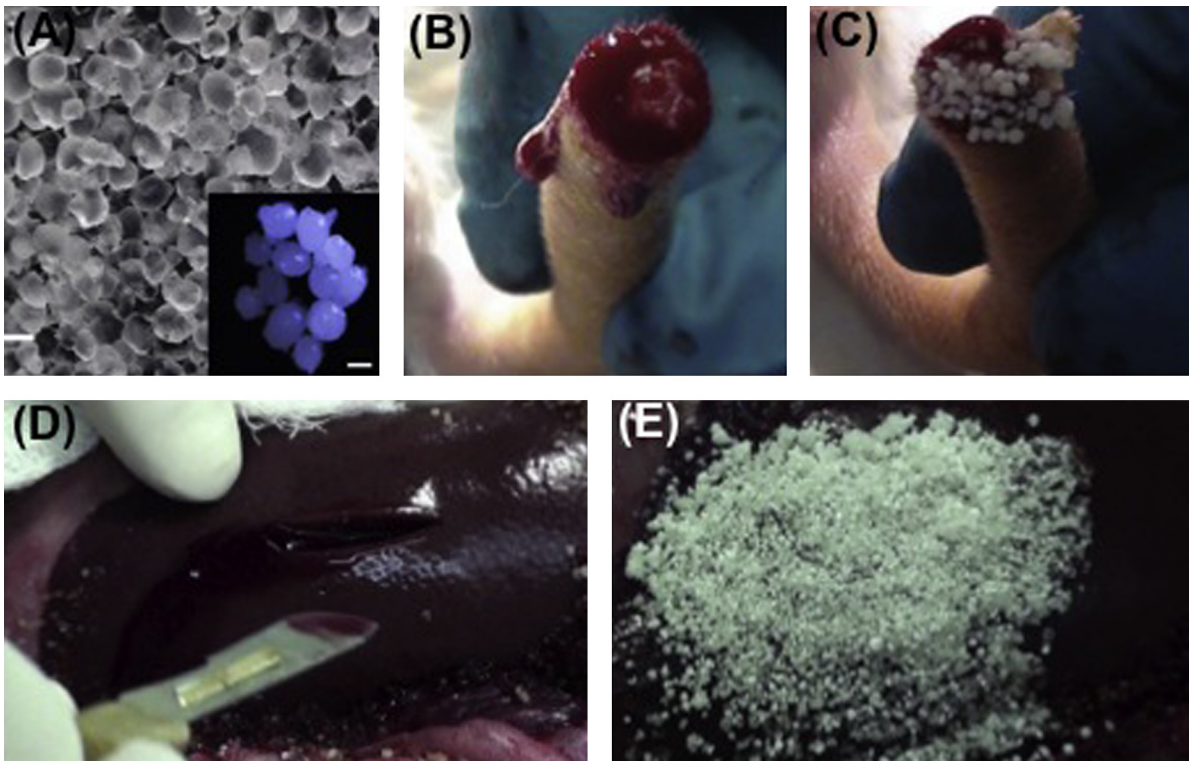

Figure 1 Fabrication of hemostatic cationic hydrogel particles. (A) N-(3-aminopropyl)methacrylamide (APM) hydrogel particles as hemostatic agents (scale bar: 5 mm in the SEM image and 500 μm in the inset). Images of a rat tail amputation (B) 5 min after applying gauze showing bleeding and (C) 5 min after applying hydrogel particles showing bleeding was stopped. (D) Image from a rat liver laceration incision, showing bleeding. (E) Image from hydrogel particles applied on liver, showing complete hemostasis (reprinted from Ref. [105]).

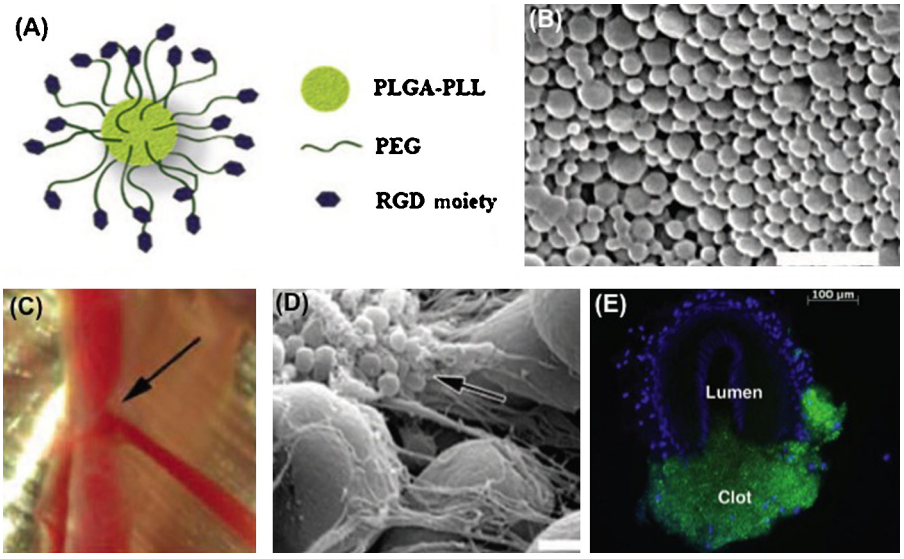

Figure 2 Engineering synthetic nanoparticles with hemostatic properties. (A) Schematic of hemostatic nanoparticles made of PLGA-PLL core with PEG arms terminated with the RGD. (B) SEM micrograph of nanoparticles (scale bar: 1 μm). (C) Femoral artery injury model used to assess the *in vivo* function of hemostatic nanoparticles, arrow shows the injury site. (D) SEM image of clot formed in an injured artery after the administration of nanoparticles, arrow shows the clot and fibrin mesh (scale bar: 1 μm). (E) Cross section view of clot following artery injury and applying coumarin 6 (C6)-labeled nanoparticles (blue: DAPI-stained cell nuclei; green: C6 from synthetic platelets within the clot) (reprinted from Ref. [106]).

Hemostatic materials with nanofibrous structures have been also developed for clinical applications [110,111]. For example, Gu et al. produced chitosan-based nanofibrous hemostatic mats with no acidic residual by using an electrospinning technique followed by neutralization [110]. The intrinsic cationic properties of chitosan and its nonspecific binding to cell membrane led to the blood protein adhesion, activation of platelets, and clot formation. The engineered electrospun chitosan sheets were neutralized in various alkali solutions after electrospinning to form non-acidic hemostatic mats. The blood clotting efficiency of these nanofibrous hemostats, with fiber diameter in the range of 350—440 nm, were then evaluated *in vitro*. The adhesion of platelets and clot formation were higher on the nanofibrous chitosan mats compared to both Surgicel (an oxidized cellulose-based hemostatic agent) and chitosan sponges [110]. Similarly, Luo et al. produced nanofibrous hemostatic material based on self-assembling chiral peptide d-EAK16 [111]. *In vitro* erythrocyte aggregation assay demonstrated the strong agglutinating activity when peptide concentration higher than 2.5 mg/ml was used. In addition, it was shown that the nanofibrous peptides could rapidly stop bleeding from an incision in a rabbit liver model, demonstrating their suitability for clinical applications as hemostatic materials [111].

Recently, nanoparticle solutions have been used as biological tissue adhesives and hemostatic materials [22,23]. For example, aqueous solutions of various nanoparticles such as silica, carbon nanotube, and cellulose nanocrystals were used to connect pieces of hydrogels or tissues together through the addition and absorption of nanoparticle solutions between the tissue pieces. It was shown that solutions of silica nanoparticles could strongly glue two pieces of calf's liver, demonstrating the potential application of these nanoparticle solutions for surgical procedures [22]. In another recent study, silica and iron oxide nanoparticles were used as hemostatic and wound closure materials in skin and liver of a rat [23]. In this study, a polymeric film was first coated by an aqueous solution of nanoparticles to absorb nanoparticles onto its surface. The film was then placed on a bleeding liver section. It was shown that particle nanobridging could provide rapid adhesion and hemostasis on the bleeding liver tissue [23]. These studies together demonstrate that merging nanotechnology with advanced tissue adhesives plays an important role in addressing unmet clinical needs for hemostatic agents.

Antibacterial materials

With increasing concern about bacterial infections in the injured sites, there is a growing need for the development of tissue adhesives with antibacterial properties. Nanoparticles have been used as antibacterial agents for many clinical applications due to their antibacterial effects on both gram negative and gram positive bacteria [112]. Antibacterial nanoparticles are classified into three groups including inorganic materials (*e.g.* metals [113], metal oxides [114], metal salts [115]), organic nanocarrier (*e.g.* polymer and lipid) loaded with antibacterial agents [116], and hybrid materials [117]. Several methods such as chemical, physical, and biological synthesis have been used to produce antibacterial nanoparticles for various clinical applications. It has been shown that the stability, size, shape, morphology, and functionalization of these nanoparticles significantly affect their antibacterial activities [118].

Antibacterial nanoparticles have been widely used as dental adhesives. For example, the addition of 10%(w/v) ZnO nanoparticles into dental composites was shown to reduce the bacterial growth around 80%. Nanocomposite dental adhesives composed of silver nanoparticles, ammonium dimethacrylate, and calcium phosphate nanoparticles were also developed to facilitate mineralization and bacterial reduction [119]. It was shown that the fabricated antibacterial nanocomposites decreased the metabolic activity of *Streptococcus mutans* biofilms [119]. Similarly, antibacterial nanocomposite adhesives based on calcium phosphate nanoparticles, calcium fluoride nanoparticles, and chlorhexidine were engineered to reduce the *S. mutans* biofilm production and lactic acid formation [120]. In another study, Ruiz et al. investigated the effect of nanoparticle size on antibacterial activity of dental adhesive against *S. mutans* [121]. They found that decreasing the size of nanoparticles from 98 nm to 9 nm significantly reduced the growth of bacteria [121].

In a recent study, Li et al. used a rat tooth cavity model to investigate the antibacterial activity and remineralizing restoration of an antibacterial bioadhesive containing calcium phosphate nanoparticles and antibacterial dimethylaminododecyl methacrylate (DMADDM) [122]. It was found that the bioadhesives containing both calcium phosphate and DMADDM had lower inflammatory response and tertiary dentin formation compared to control groups without or with one type of nanoparticles. The presence of calcium phosphate nanoparticles in these composites reduced inflammation and enhanced tissue formation and the addition of DMADDM into composites promoted antibacterial activity with no adverse effect on pulpal response [122]. In another study, Melo et al. developed antibacterial dental adhesives containing calcium phosphate and silver nanoparticles. The fabricated dental adhesives enhanced bonding strength to dentin and inhibited bacterial growth and acid production in tooth cavity [123]. It was also found that incorporation of silver nanoparticles and calcium phosphate into adhesive had no adverse effects on the bonding strength but significantly enhanced antibacterial activities and remineralization of tooth lesions [123].

Antibacterial nanoparticles have been also incorporated into tissue adhesives for wound protection and healing [115,124]. For example, nanocomposites composed of genipin-crosslinked chitosan (GC), PEG, ZnO, and silver nanoparticles were synthesized and used as antibacterial tissue adhesives for wound healing [124]. It was shown that the nanocomposites contained silver nanoparticles had higher antibacterial activity compared with those without silver nanoparticles [124]. In another study, Buckley et al. showed that silver impregnated mesoporous hydroxyapatite enhanced the production of silver phosphate antibacterial nanoparticles against two bacteria, *Staphylococcus aureus* and *Pseudomonas aeruginosa*, commonly present on the wounds and skin [115]. Silver nanoparticles conjugated glucose and glycosaminoglycan were also used as antibacterial bioadhesives for wound closing or as an antibacterial coating on surgical tools and catheter [125]. In another study,

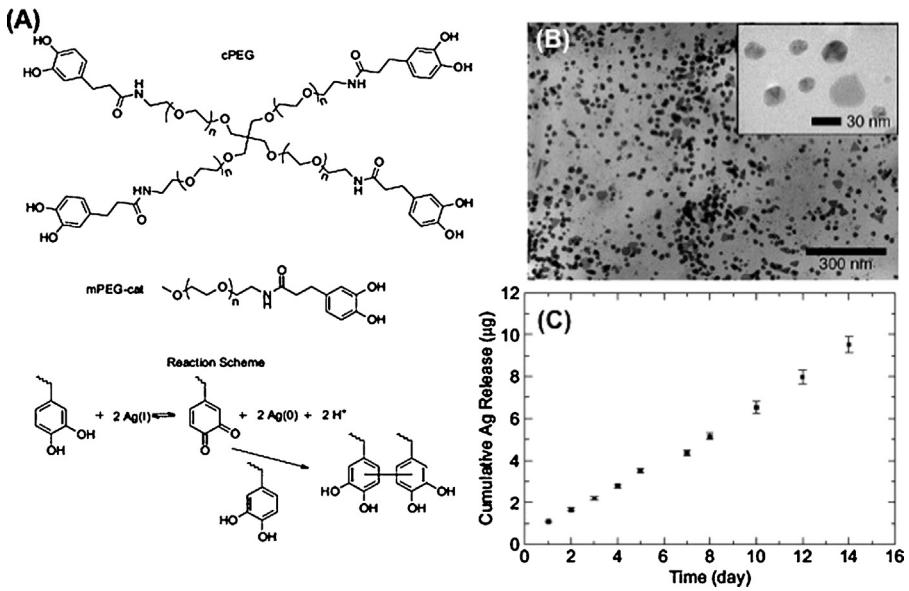

Figure 3 Development of an antibacterial hydrogel-based tissue adhesive. (A) Synthesis of an antibacterial hydrogel based on a branched catechol functionalized PEG and silver ion. (B) TEM images of silver nanoparticles formed through the reaction between silver ion and catechol functionalized PEG. (C) Cumulative silver release from the fabricated antibacterial hydrogel over two weeks (reprinted from Ref. [132]).

antibacterial agents based on silver nanoparticle incorporated hyaluronan fibers were formed for wound closure and healing [126]. Hyaluronan fibers were first formed by using a wet spinning technique. The fibers were then used as a capping and stabilizing agent to create silver nanoparticles through a chemical reduction of sliver nitrate. The engineered fibers containing silver nanoparticles exhibited strong antibacterial activity against *S. aureus* and *Escherichia coli*, demonstrating their capability for utilization as wound dressing bioadhesives [126]. In a recent study, Wu et al. synthesized an antibacterial wound dressing through the impregnation of silver nanoparticles on cellulose nanofibers. The engineered nanocomposite induced 99% reduction in *P. aerudomonas*, *S. aureus* and *E. coli*, demonstrating its high antibacterial activity. The results of *in vitro* studies also confirmed that silver nanoparticle incorporated cellulose composites had no cytotoxicity to cells, demonstrating their suitability as tissue adhesives for wound dressing [127]. In another study, Guo et al. developed an antibacterial bioadhesive for ocular treatment by incorporating moxifloxacin loaded poly(lactic-co-glycolic acid) (PLGA) microparticles in a chondroitin sulfate (CS)/PEG hydrogel [128]. Moxifloxacin incorporated PLGA nanoparticles with diameter less than 1 μm were produced by using an electrospraying technique. The particles were then loaded in CS/PEG hydrogel to form a bioadhesive containing antibacterial particles with a controlled release rate of up to 10 days. The developed antibacterial bioadhesive showed great potential to be used as an antibiotic delivery for wound healing in the eye [128].

Nanofibrous materials with antibacterial properties have also been used as adhesive biomaterials for clinical applications such as wound dressings. The antibacterial properties may stem from the employed polymers or from the incorporated antibacterial reagents. For example, Lakshman et al. fabricated nanofibrous PU substrates containing silver nanoparticles as an antibacterial wound dressing platform [129]. In addition to suitable exudates management properties, the fabricated substrates could prevent the growth of *Klebsiella*. In another example, Shalumon et al. fabricated alginate/poly(vinyl alcohol) nanofibrous mats loaded with ZnO nanoparticles [130]. The embedded ZnO nanoparticles could inhibit the growth of *S. aureus* and *E. coli*. In another instance, Cai et al. electrospun a mixture of chitosan and silk fibroin to create nanofibrous substrates with antibacterial properties for wound dressings [131]. The antibacterial activity of the fabricated substrates was assessed against cultures of *S. aureus* and *E. coli*.

Inspired by mussel adhesive proteins, Fullenkamp et al. recently synthesized an antibacterial hydrogel by using silver for spontaneous hydrogel formation through catechol oxidation (Figure 3A) and as a precursor for the formation of silver nanoparticles to give antibacterial properties to the formed hydrogel [132]. Catechol containing PEG was used to form the hydrogel and the polymer catechols were oxidized by silver titrate for simultaneous hydrogel curing and reduction of silver ion. These reactions resulted in the formation of round-shape nanoparticles with diameters that were up to 50 nm (Figure 3B). It was found that silver release from the hydrogel was sustained for at least two weeks in aqueous solution (Figure 3C). The engineered antibacterial hydrogel was shown to kill bacteria cells without reducing the viability of mammalian cells, demonstrating its capability to be used as antibacterial tissue adhesives [132].

In a recent study, the mechanism of antibacterial activity of ionic silver against Gram-negative bacteria was investigated [133]. The result of *in vitro* and *in vivo* tests showed that silver disrupted multiple bacterial cellular processes, which led to an increase in the formation of reactive oxygen species and membrane permeability permeation of the Gram-negative bacteria [133]. In addition, the toxicity of ionic silver *in vivo* was studied by determining a median

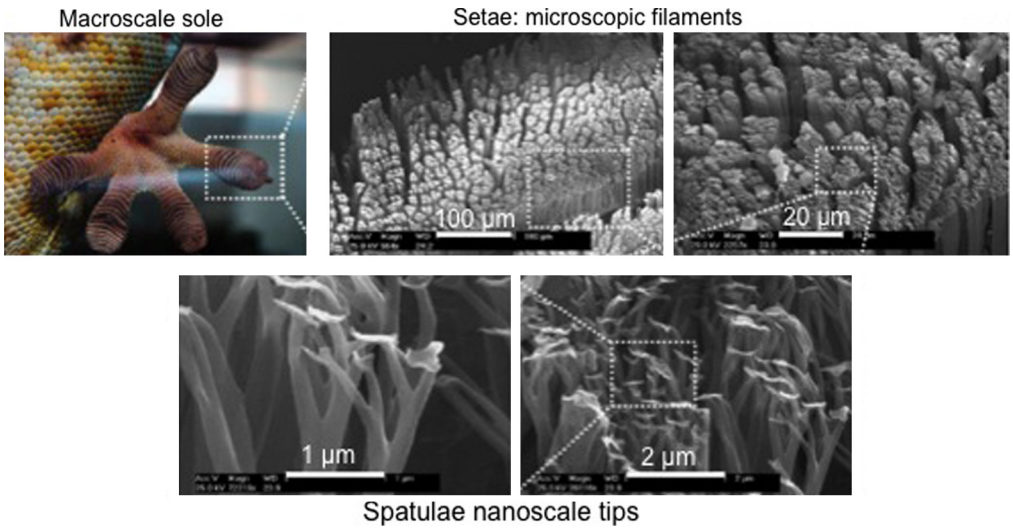

Figure 4 Hierarchical topography of geckos sole. The topography is formed from microscale filament (setae), which branch into nanoscale tips with mushroom-like heads (reprinted from Ref. [137]).

lethal dose (LD50) between 120 and 240 μM. The use of silver nanoparticles for the development of antibacterial tissue adhesives has attracted significant attention due to their effective antibacterial activity. However, their potential toxicity should be considered for clinical applications.

Biomimetic nanostructured surgical materials

Living organisms have evolved over millions of years to acquire skills to adapt to the environmental conditions and to enhance their survival chance among other creatures. Nature is filled with examples such as mussels, lizards, and insects that rely on efficient adhesion to wet or dry surfaces for survival [134]. These natural models have been inspiring scientists to develop new materials and strategies to fabricate more effective tissue adhesives. In the previous sections, we discussed some of the naturally inspired materials such as mussel protein adhesives and DOPA-based glues. In this section, we will focus on the strategies that utilize biomimetic nanotopography to enhance the adhesion force between the engineered tissue adhesives and the surrounding tissues.

The reversible adhesion of gecko lizards to dry and rough surfaces has fascinated scientists to understand this adhesion mechanism and then adopt a similar strategy to design dry adhesives [135,136]. Gecko's soles contain arrays of microscale fibers (setae) which in turn are split into mushroom-tipped nanoscale fibrils (spatula) to form a hierarchical structure (Figure 4) [137]. A combination of van der Waals and capillary forces at the contact area between spatula and surface creates strong reversible adhesion (up to 10 N/cm^2) [138]. To mimic these structures, micro and nanotechnologies have been utilized over the past few years to create highly adherent surfaces [139]. Creating a gecko-inspired topography requires a combination of the following characteristics: (i) high aspect ratio structures (AR > 10); (ii) slanted features to create anisotropic adhesion; (iii) structures with spatulate head; and (iv) hierarchical structures. In addition, the employed materials should be flexible to allow an increased contact area between the adhesive patch and rough surfaces.

Murphy et al. also fabricated a hierarchical topography on the surface of a PU patch with an elastic modulus of 3 MPa [140]. The PU surface was covered with slanted mushroom head tipped microposts with 35 μm tip diameter and 100 μm long (Figure 5 A–C). Their results indicated highly anisotropic behavior for posts with slanted tips. They demonstrated that 1 cm^2 of the patch could hold 1 kg weight (~10 N/cm^2) in the gripping direction (Figure 5D) [140]. In another study, the same group fabricated a PU patch with microscale slanted posts (600 μm tip diameter and 1.2 mm long) where their tips were covered by smaller posts (112 μm tip diameter and 100 μm long) [141]. They compared the adhesion force of patches containing double level topography with the values for patches with and without single level posts (Figure 5E). Their results suggested that the hierarchical structure increased the adhesion force by almost six folds [141]. In another study, Jeong et al. fabricated poly(urethane acrylate) (PUA) nanoscale fibrils through replica molding with mushroom-like tips [142]. Due to the formation of nanosized topography, they achieved a shear adhesion of 25 N/cm^2, which was 10 times higher than those reported by Murphy et al. Jeong et al. also combined molding and surface wrinkling to create stretchable and reversibly adhesive surfaces. They created poly(dimethylsiloxane) (PDMS) sheets covered with posts through molding and then covered the tips with UV crosslinkable PUA. They could achieve adhesion strength of ~11 N/cm^2 which was reversible and remained almost constant over 100 cycles of attachment and detachment [24].

The major difference between the operation of wet adhesives and the dry adhesives discussed above is the wet tissue environment in which gecko-inspired surfaces cannot adhere. In addition, tissue adhesives are meant to be long lasting and have irreversible adhesion to the tissues. Lee et al. developed the first gecko-inspired wet and dry adhesives in which the surface of fibrous topography was

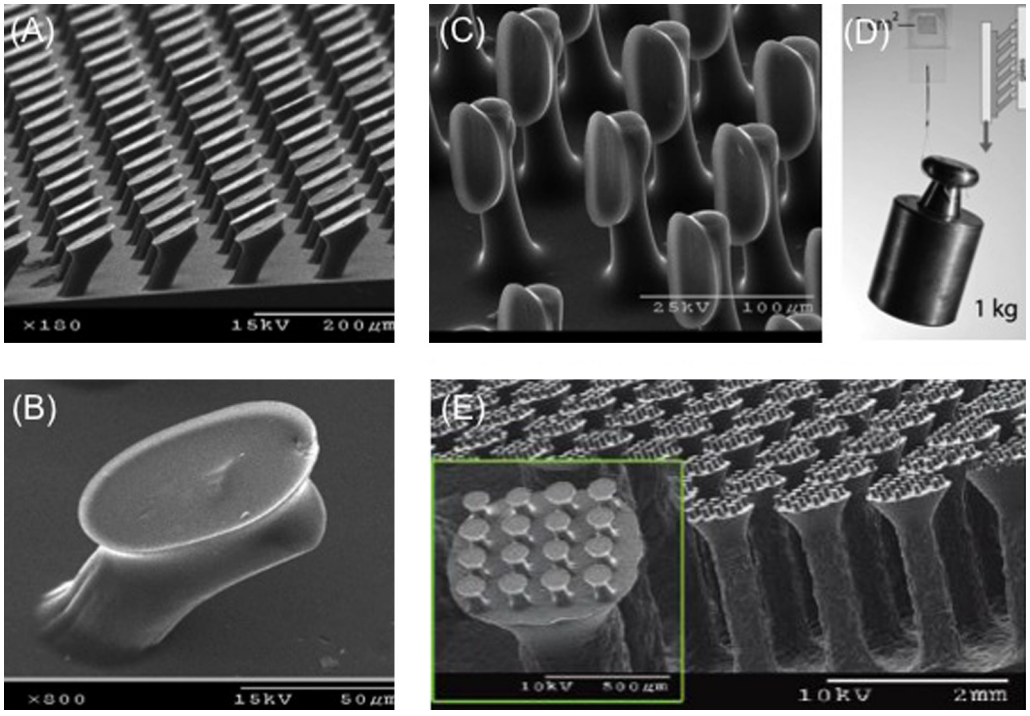

Figure 5 SEM images of gecko-inspired surfaces. (A—C) Angled polyurethane (PU) posts with angled mushroom tips. The tip orientation was changed at different angles: (A) 34°; (B) 23°; (C) 90°; (D) 1 cm^2 PU patch covered with angled posts supported 1 kg weight (reprinted from Ref. [140]). (E) Two-level PU posts fabricated using molding to create hierarchical topography (reprinted from Ref. [141]).

coated by poly(dopamine methacrylamide-co-methoxyethyl acrylate) (pDMA-co-MEA) to mimic the adhesion mechanism of mussels [66]. The patch was made from PDMS covered with fibrils of 400 nm in diameter and 600 nm in length. The adhesion force of pDMA-co-MEA coated fibrils in wet condition was reported to be 86.3 nN in comparison to the value of 5.9 nN for the non-coated ones. Glass et al. investigated synergic effect of surface topography and coating with DOPA-based polymers for adhesion under wet conditions. They found that the DOPA-coating increased the

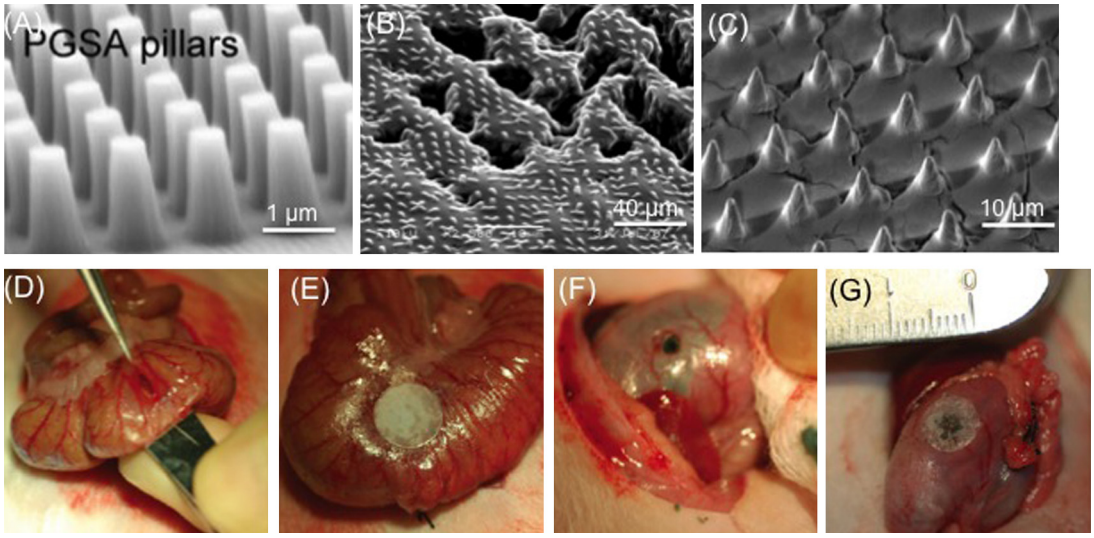

Figure 6 Gecko-inspired bioadhesives. (A) SEM images of a PGSA patch with nanopillars. (B) PGSA patch after 8 days of implantation which confirms the stability of nanopillars *in vivo* (reprinted from Ref. [144]). (C) SEM image of PCL patch with micropillars coated with cyanoacrylate. (D) A 3 mm diameter puncture in a rat colon. (E) Closure of the punctured region with the PCL patch. (F) Image of a 3 mm defect created in rat stomach. (G) Successful implementation of the PCL patch for closing the defect (reprinted from Ref. [145]).

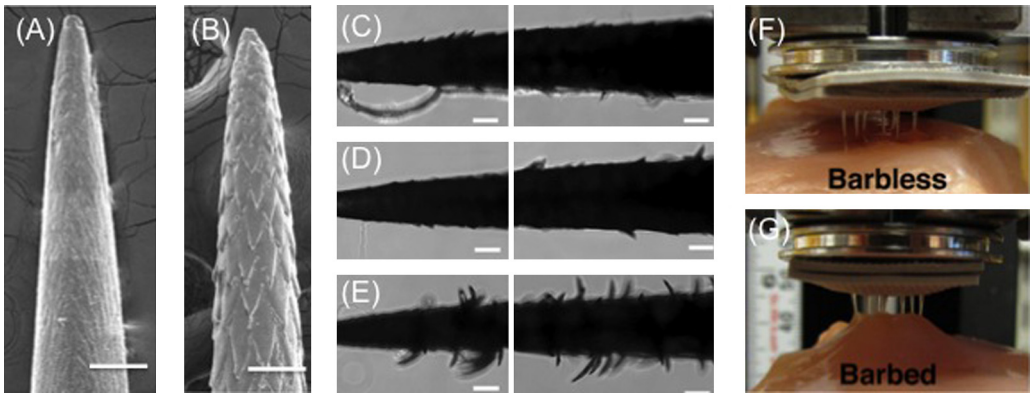

Figure 7 Porcupine quill-inspired tissue adhesives. (A, B) SEM images of barbless and barbed polyurethane quills (scale bar 500 μm). (C—E) Images showing the quills surface topography after removal from porcine skin. The topography creates mechanical interlocking, which increases the pullout force of the quills from the skin (scale bar: 500 μm). (F,G) Adhesion test of a patch containing barbless and barbed quills to porcine skin. The barbed quills improve the path attachment through mechanical interlocking (reprinted from Ref. [149]).

adhesion force by two folds [143]. Mahdavi et al. developed another gecko-inspired tissue adhesive by generating nanosized posts with diameters ranging from 100 nm to 1 μm and heights of 0.8—3 μm on the surface of PGSA using a molding process (Figure 6A) [144]. The surface of the fabricated patterns was coated by a thin layer of oxidized dextran aldehyde (DXT) to promote bonding to the tissue. Shear adhesion tests on patterned PGSA and porcine intestinal tissue showed a maximum separation force of 4.8 N/cm^2 which was almost double of the value for flat PGSA substrate. Their *in vivo* tests for the gecko-inspired patches after two days of implantation indicated an adhesion force of 0.7 N/cm^2 (Figure 6B). It was also shown that the conformal contact between the adhesive patch and the tissue could improve by increasing the distance between the posts, which was somehow in contrast with their inspiration from gecko soles [144]. Furthermore, in another example, Pereira et al. fabricated PCL patches covered with microposts (base: 4.9 μm, length: 19.0 μm, pitch: 9.5 μm, Figure 6C) [145]. A layer of cyanoacrylate medical glue was then spin coated on the patterned patch. The adhesion force of the patterned patches (~2.5 N/cm^2) was 2.6 times higher than the value for unpatterned ones (~1 N/cm^2). A minimal inflammatory response was observed following three weeks implantation of the fabricated nanopatterned patch in a rat model. The patch was also used for closing colon and stomach punctures in rats (Figure 6D—G) [145]. In another study, Martinelli et al. fabricated buckypapers (BP) with a highly porous fibrous microstructure from multi-walled carbon nanotubes (MWCNTs) [146]. The material was very hydrophilic and its surface was quite rough with a maximum roughness height of 400 nm. They measured the shear adhesion strength of the fabricated BP to a biological tissue, which was 20 mN/mm^2. This value was comparable to the values for the gecko-inspired patch developed by Mahdavi et al. [144]. The high mechanical adhesion was related to the material hydrophilicity which enhanced the capillary forces, high porosity, and surface topography [146].

Gecko-inspired surfaces have also been used for designing tissue adhesive drug releasing capsules. In a recent study, Fischer et al. grew silicon nanowires (60 nm diameter) on the surface of 30—50 μm diameter glass beads to increase their adhesion to mucosal epithelia [147]. In addition to an increase in the van der Waals interaction between the particle surface and the tissue due to presence of the nanotopography, the presence of nanostructured microvilli on the tissue could potentially further enhance the adhesion strength. Upon incubation of coated and non-coated beads with cells, authors reported almost three times higher adherence due to nanotopography. The results suggested that the use of nanopatterned microcapsules could potentially enhance the drug delivery efficiency [147].

Bio-inspired adhesives are not limited to gecko-based surfaces. There are many examples of living organisms, which rely on strong attachment to surfaces. For example, *Pomphorhynchus laevis* is an endoparasite which inserts its proboscis into the intestine wall of the host fish and swells them to create high adhesion strength. This observation inspired Yang et al. to fabricate a tissue adhesive containing microneedles with swellable tips to mechanically interlock with native tissue [148]. To form the patch, a polystyrene (PS) core was first covered with a layer of swellable polystyrene-block-poly(acrylic acid) (PS-bPAA). Upon insertion of the needles into the tissue, the tip absorbed liquid and swelled to mechanically interlock within the tissue. The *in vivo* tests on the rat skin showed that the swellable tips increased the removal force by seven times (1.2 N/cm^2) in comparison to the patches with regular PS needles. The maximum adhesion strength to the intestinal mucosal tissue was reported 4.5 N/cm^2 which was 3.5 times higher than the values for surgical staples. Moreover, the swellable needles eliminated the chance of bacterial infiltration into the punctured hole which is a major challenge in the use of surgical staples [148].

To develop biomimetic tissue adhesives, Cho et al. mimicked the topography and shape of North American porcupine quills tip that contains microscopic backward facing barbs (Figure 7A and B). They determined that the penetration force for barbed quills was 54% less than the value for barbless quills while its pull out force was three times higher [149]. The increase in the pull-out force was

due to mechanical interlocking of the barbs into the tissue. They fabricated PU barbed and barbless quills through micromolding and the barbed ones required 35% less penetration force. They also observed a correlation between the pull-out force and the number of dislocated barbs (Figure 7C–E). Based on the easy tissue penetration and strong adhesion force of the barbed quills, Cho et al. fabricated a biomimetic tissue adhesive containing an array of microneedles. The fabricated PU patches with barbed microneedles had a pull-out force of four times higher than those with barbless needles and could maintain their conformal contact to the tissue (Figure 7F and G) [149].

In another example, Tsai and Chang investigated the adhesion mechanism of water beetles to wet surfaces to design auto-adhesive transdermal drug delivery patches [150]. They fabricated PDMS patches with microposts of 2 μm in diameter and 2 μm in height. To mimic the secretion by the insect to enhance the adhesion, they loaded silicon oil within the PDMS molds and showed that an adhesion force of 9.5 N/cm^2 (normal load) and 5.0 N/cm^2 (sheer load) was achieved. The tissue adhesives discussed in this section can be potentially used for closing punctures or wounds during open surgeries, however, their utilization in minimally invasive surgeries is extremely challenging. Also, the significant difference between the elastic modulus of the fabricated patches and various soft tissues is another important challenge, which can prevent effective healing of the damaged tissues. Although the use of other biocompatible materials such as hydrogels which possess mechanical characteristics similar to soft tissues can potentially solve this challenge, the fabrication of high aspect ratio feature in soft materials is extremely challenging.

Conclusion and future direction

During the last decades, synthetic or biological tissue adhesives that rely on *in situ* polymerizations and crosslinking reactions have emerged as complementary techniques and could address many challenges associated with sutures and staples particularly in noninvasive surgeries. However, currently available tissue adhesives for clinical applications have some limitations including toxicity, extensive swelling, insufficient strength, and complex polymerization process. In addition, the use of these polymer-based surgical materials requires specific storage and preparation conditions before applying *in vivo*.

Recent advancements in nanotechnologies have touched the field of tissue adhesives by either introducing new functionalities (*e.g.* hemostatic or antibacterial properties) or improving their mechanical properties as well as their adhesion force to surrounding tissues. For example, recently it has been shown that aqueous solution of nanoparticles can act as connector to strongly bond tissue pieces together. Rapid and strong adhesion by nanoparticle solutions can be advantageous in very different clinical situations. For instance, nanoparticle solutions can be easily applied for wound closure and healing without the need for any specific preparation or training. Nanoparticle solutions can be also used to control bleeding in liver, kidney, and heart surgeries. In addition, nanoparticles with antibacterial and hemostatic properties have been incorporated into polymeric adhesives to reduce the risk of infections or hemorrhage after surgeries. Tissue adhesives can potentially carry and release various drugs at the injury site to facilitate the healing process and tissue regeneration as well as to control the inflammatory response. The utilization of drug nanocarriers such as liposomes and nanoparticles allows prolonged and sequential delivery of various drugs and factors. Therefore, it is anticipated that by using such nanocarriers, multifunctional tissue adhesives can be synthesized, which are specialized for a targeted tissue.

Creating artificial nanotopography that is inspired by observations from nature has enabled scientist to create tissue adhesive patches with high adhesion properties. These patches are prefabricated and can be used in a wide range of open surgical operations. As a result, such patches cannot be employed in laparoscopic surgeries or in blocking intrusions with severe hemorrhage. One potential direction of the field is to create injectable adhesives that can crosslink *in situ* and form nanotopography to enhance their adhesion to surrounding tissues through van der Waals interaction or mechanical interlocking.

Recent developments in nanofabrication techniques have significantly contributed to the emergence of the field of flexible and biodegradable electronics. One potential future direction can be to combine polymeric tissue adhesives with biodegradable electronics [151,152] to create smart tissue adhesive. Such smart adhesive can monitor the healing process and the injury site environment for potential infections and inflammations. Overall it is expected that by the new functionalities added to tissue adhesives, they will be more popular and can replace surgical staples and sutures in a wide range of operations.

Acknowledgments

N.A. acknowledges the support from the National Health and Medical Research Council (NHMRC, APP1037349). A.K. acknowledges funding from the National Science Foundation CAREER Award (DMR 0847287), the office of Naval Research Young National Investigator Award, the National Institutes of Health (HL092836, DE019024, EB012597, AR057837, DE021468, HL099073, EB008392), and the Presidential Early Career Award for Scientists and Engineers (PECASE). A.T. acknowledges the financial support of the Natural Sciences and Engineering Research Council of Canada (NSERC). NAP acknowledges funding from the National Science Foundation (CBET1033746) and the National Institutes of Health (EB00246, EB012726) and the Gates Foundation (1007287).

References

[1] P. Ferreira, R. Pereira, J.F.J. Coelho, A.F.M. Silva, M.H. Gil, Int. J. Biol. Macromol. 40 (2007) 144–152.
[2] C.L. Oliveira, C.H.M. Santos, F.M.M. Bezerra, M.M. Bezerra, L.L. Rodrigues, Rev. Bras. Cir. Plást. 25 (2010) 573–576.
[3] S. Suzuki, Y. Ikada, Biomaterials for Surgical Operation, Springer, New York, 2012.
[4] J.B. Thomas, N.A. Peppas, in: G.E. Wnek, G.L. Bowlin (Eds.), Encyclopedia of Biomaterials and Biomedical Engineering, Dekker, New York, 2006.
[5] H.T. Peng, P.N. Shek, Expert Rev. Med. Devices 7 (2010) 639–659.

[6] A.P. Duarte, J.F. Coelho, J.C. Bordado, M.T. Cidade, M.H. Gil, Prog. Polym. Sci. 37 (2012) 1031—1050.
[7] J. Brand, S. Gruber-Blum, K. Gruber, R.H. Fortelny, H. Redl, A.H. Petter-Puchner, J. Surg. Res. 183 (2013) 726—732.
[8] M.A. Carlson, J. Calcaterra, J.M. Johanning, I.I. Pipinos, C.M. Cordes, W.H. Velander, J. Surg. Res. 187 (2014) 334—342.
[9] S.H. Baik, J.H. Kim, H.H. Cho, S.-N. Park, Y.S. Kim, H. Suh, J. Surg. Res. 164 (2010) e221—e228.
[10] C.M. Elvin, T. Vuocolo, A.G. Brownlee, L. Sando, M.G. Huson, N.E. Liyou, P.R. Stockwell, R.E. Lyons, M. Kim, G.A. Edwards, G. Johnson, G.A. McFarland, J.A.M. Ramshaw, J.A. Werkmeister, Biomaterials 31 (2010) 8323—8331.
[11] A. Lauto, L.J. Foster, A. Avolio, D. Sampson, C. Raston, M. Sarris, G. McKenzie, M. Stoodley, Photomed. Laser Surg. 26 (2008) 227—234.
[12] Y.M. Bhat, S. Banerjee, B.A. Barth, S.S. Chauhan, K.T. Gottlieb, V. Konda, J.T. Maple, F.M. Murad, P.R. Pfau, D.K. Pleskow, U.D. Siddiqui, J.L. Tokar, A. Wang, S.A. Rodriguez, Gastrointest. Endosc. 78 (2013) 209—215.
[13] J. Sageshima, G. Ciancio, K. Uchida, A. Romano, Z. Acun, L. Chen, G.W. Burke Iii, Transplant. Proc. 43 (2011) 2584—2586.
[14] C.S. Johnson, M. Wathier, M. Grinstaff, T. Kim, Arch. Ophthalmol. 127 (2009) 430—434.
[15] T.W. Gilbert, S.F. Badylak, E.J. Beckman, D.M. Clower, J.P. Rubin, J. Plast. Reconstr. Aesthet. Surg. 66 (2013) 414—422.
[16] J.C. Wain, L.R. Kaiser, D.W. Johnstone, S.C. Yang, C.D. Wright, J.S. Friedberg, R.H. Feins, R.F. Heitmiller, D.J. Mathisen, M.R. Selwyn, Ann. Thorac. Surg. 71 (2001) 1623—1629.
[17] H. Nomori, H. Horio, S. Morinaga, K. Suemasu, Ann. Thorac. Surg. 67 (1999) 212—216.
[18] C. Fuller, J. Cardiothorac. Surg. 8 (2013) 90.
[19] T. Wang, X. Mu, H. Li, W. Wu, J. Nie, D. Yang, Carbohydr. Polym. 92 (2013) 1423—1431.
[20] W. Nie, X. Yuan, J. Zhao, Y. Zhou, H. Bao, Carbohydr. Polym. 96 (2013) 342—348.
[21] C. Li, T. Wang, L. Hu, Y. Wei, J. Liu, X. Mu, J. Nie, D. Yang, Mater. Sci. Eng. C 35 (2014) 300—306.
[22] S. Rose, A. Prevoteau, P. Elziere, D. Hourdet, A. Marcellan, L. Leibler, Nature 505 (2014) 382—385.
[23] A. Meddahi-Pellé, A. Legrand, A. Marcellan, L. Louedec, D. Letourneur, L. Leibler, Angew. Chem. Int. Ed. Engl. 53 (2014) 6369—6373.
[24] H.E. Jeong, M.K. Kwak, K.Y. Suh, Langmuir 26 (2010) 2223—2226.
[25] X. Mo, H. Iwata, Y. Ikada, J. Biomed. Mater. Res. A 94 (2010) 326—332.
[26] A.J. Singer, H.C. Thode Jr., Am. J. Surg. 187 (2004) 238—248.
[27] A.J. Singer, J.V. Quinn, J.E. Hollander, Am. J. Emerg. Med. 26 (2008) 490—496.
[28] N. Annabi, A. Tamayol, J.A. Uquillas, M. Akbari, L.E. Bertassoni, C. Cha, G. Camci-Unal, M.R. Dokmeci, N.A. Peppas, A. Khademhosseini, Adv. Mater. 26 (2014) 85—124.
[29] M. Mehdizadeh, J. Yang, Macromol. Biosci. 13 (2013) 271—288.
[30] D.H. Sierra, J. Biomater. Appl. 7 (1993) 309—352.
[31] H.G. Borst, A. Haverich, G. Walterbusch, W. Maatz, J. Thorac. Cardiovasc. Surg. 84 (1982) 548—553.
[32] Y. Sawamura, K. Asaoka, S. Terasaka, M. Tada, T. Uchida, Neurosurgery 44 (1999) 332—337.
[33] D.H. Sierra, A.W. Eberhardt, J.E. Lemons, J. Biomed. Mater. Res. 59 (2002) 1—11.
[34] Y. Ikada, Aborbable hydrogels for medical use, in: Y. Osada, K. Kajiwara, T. Fushimi, O. Irasa, Y. Hirokawa, T. Matsunaga, T. Shimomura, L. Wang, H. Ishida (Eds.), Gels Handbook, Academic Press, USA, 2000.
[35] W.D. Spotnitz, J.K. Falstrom, G.T. Rodeheaver, Surg. Clin. North Am. 77 (1997) 651—669.
[36] W.G. Schenk Iii, S.G. Burks, P.J. Gagne, S.A. Kagan, J.H. Lawson, W.D. Spotnitz, A.F. Aburahma, W.G. Schenk Iii, Ann. Surg. 237 (2003) 871—876.
[37] M. Hino, O. Ishiko, K.I. Honda, T. Yamane, K. Ohta, T. Takubo, N. Tatsumi, Br. J. Haematol. 108 (2000) 194—195.
[38] T.B. Reece, T.S. Maxey, I.L. Kron, Am. J. Surg. 182 (2001) S40—S44.
[39] K.L. Renkens Jr., T.D. Payner, T.J. Leipzig, H. Feuer, M.A. Morone, J.M. Koers, K.J. Lawson, R. Lentz, H. Shuey Jr., G.L. Conaway, G.B.J. Andersson, H.S. An, M. Hickey, J.F. Rondinone, N.S. Shargill, Spine 26 (2001).
[40] W.C. Chapman, R. Sherman, S. Boyce, M. Malawer, A. Hill, G. Buncke, J.E. Block, J.J. Fung, P. Clavien, K.F. Lee, G.S. Lebovic, S.M. Wren, E. Diethrich, R. Goldsein, Surgery 129 (2001) 445—450.
[41] D.I. Lee, C. Uribe, L. Eichel, S. Khonsari, J. Basillote, H.K. Park, C.C. Li, E.M. McDougall, R.V. Clayman, J. Urol. 171 (2004) 575—578.
[42] T. Chen, R. Janjua, M.K. McDermott, S.L. Bernstein, S.M. Steidl, G.F. Payne, J. Biomed. Mater. Res.: B Appl. Biomater. 77 (2006) 416—422.
[43] V.Y. Sohn, M.J. Eckert, M.J. Martin, Z.M. Arthurs, J.R. Perry, A. Beekley, E.J. Rubel, R.P. Adams, G.L. Bickett, R.M. Rush Jr., J. Surg. Res. 154 (2009) 258—261.
[44] B.G. Kozen, S.J. Kircher, J. Henao, F.S. Godinez, A.S. Johnson, Am. J. Emerg. Med. 15 (2008) 74—81.
[45] M. Kirsch, M. Ginat, L. Lecerf, R.m. Houël, D. Loisance, Ann. Thorac. Surg. 73 (2002) 642—644.
[46] H. Tsukui, S. Aomi, H. Nishida, M. Endo, H. Koyanagi, Ann. Thorac. Surg. 72 (2001) 1733—1735.
[47] M. Miscusi, Spine. J. 11 (2011) 983.
[48] G. Hidas, A. Kastin, M. Mullerad, J. Shental, B. Moskovitz, O. Nativ, Urology 67 (2006) 697—700.
[49] J. Passage, H. Jalali, R.K.W. Tam, S. Harrocks, M.F. O,ÄôBrien, Ann. Thorac. Surg. 74 (2002) 432—437.
[50] M.M. Saunders, Z.C. Baxter, A. Abou-Elella, A.R. Kunselman, J.C. Trussell, Fertil. Steril. 91 (2009) 560—565.
[51] L. Montanaro, C.R. Arciola, E. Cenni, G. Ciapetti, F. Savioli, F. Filippini, L.A. Barsanti, Biomaterials 22 (2001) 59—66.
[52] T.B. Bruns, J.M. Worthington, Am. Fam. Physician 61 (2000) 1383—1388.
[53] S. Kull, I. Martinelli, E. Briganti, P. Losi, D. Spiller, S. Tonlorenzi, G. Soldani, J. Surg. Res. 157 (2009) e15—e21.
[54] A. Cannata, C. Taglieri, C.F. Russo, G. Bruschi, L. Martinelli, Ann. Thorac. Surg. 87 (2009) 1956—1958.
[55] K.E. Rodgers, F.G. Burleson, G.R. Burleson, M.J. Wolfsegger, K.M. Lewis, H. Redl, Am. J. Obstet. Gynecol. 203 (2010) 494 (e491-494. e496).
[56] P. Fransen, Spine. J. 10 (2010) 751—761.
[57] K.-L. Lin, D.-Y. Yang, I.M. Chu, F.-C. Cheng, C.-J. Chen, S.-P. Ho, H.-C. Pan, J. Surg. Res. 161 (2010) 101—110.
[58] J.W. Osbun, R.G. Ellenbogen, R.M. Chesnut, L.S. Chin, P.J. Connolly, G.R. Cosgrove, J.B. Delashaw Jr., J.G. Golfinos, J.D.W. Greenlee, S.J. Haines, J. Jallo, J.P. Muizelaar, A. Nanda, M. Shaffrey, M.V. Shah, J.M. Tew Jr., H.R. van Loveren, M.E. Weinand, J.A. White, J.E. Wilberger, World Neurosurg. 78 (2012) 498—504.
[59] D.F. Torchiana, J. Card. Surg. 18 (2003) 504—506.
[60] C.H. Alleyne Jr., C.M. Cawley, D.L. Barrow, B.C. Poff, M.D. Powell, A.S. Sawhney, D.L. Dillehay, J. Neurosurg. 88 (1998) 308—313.
[61] J.C. Wheat, J.S. Wolf Jr., Urol. Clin. North Am. 36 (2009) 265—275.
[62] T.W. Gilbert, S.F. Badylak, J. Gusenoff, E.J. Beckman, D.M. Clower, P. Daly, J.P. Rubin, Plast. Reconstr. Surg. 122 (2008) 95—102.

[63] P. Ferreira, A.F.M. Silva, M.I. Pinto, M.H. Gil, J. Mater. Sci.: Mater. Med. 19 (2008) 111—120.
[64] N. Lang, M.J. Pereira, Y. Lee, I. Friehs, N.V. Vasilyev, E.N. Feins, K. Ablasser, E.D. O'Cearbhaill, C. Xu, A. Fabozzo, R. Padera, S. Wasserman, F. Freudenthal, L.S. Ferreira, R. Langer, J.M. Karp, P.J. del Nido, Sci. Transl. Med. 6 (2014) 218ra216.
[65] K. Kamino, Mar. Biotechnol. 10 (2008) 111—121.
[66] H. Lee, B.P. Lee, P.B. Messersmith, Nature 448 (2007) 338—341.
[67] L. Serra, J. Doménech, N.A. Peppas, Eur. J. Pharm. Biopharm. 71 (2009) 519—528.
[68] J.J. Wilker, Curr. Opin. Chem. Biol. 14 (2010) 276—283.
[69] M. Yu, J. Hwang, T.J. Deming, J. Am. Chem. Soc. 121 (1999) 5825—5826.
[70] K. Yamada, T. Chen, G. Kumar, O. Vesnovsky, L.D. Timmie Topoleski, G.F. Payne, Biomacromolecules 1 (2000) 252—258.
[71] H. Tatehata, A. Mochizuki, K. Ohkawa, M. Yamada, H. Yamamoto, J. Adhes. Sci. Technol. 15 (2001) 1003—1013.
[72] B.P. Lee, J.L. Dalsin, P.B. Messersmith, Biomacromolecules 3 (2002) 1038—1047.
[73] L. Ninan, J. Monahan, R.L. Stroshine, J.J. Wilker, R. Shi, Biomaterials 24 (2003) 4091—4099.
[74] D.S. Hwang, Y. Gim, H.J. Yoo, H.J. Cha, Biomaterials 28 (2007) 3560—3568.
[75] J. Monahan, J.J. Wilker, Langmuir 20 (2004) 3724—3729.
[76] J. Wang, C. Liu, X. Lu, M. Yin, Biomaterials 28 (2007) 3456—3468.
[77] B.J. Kim, D.X. Oh, S. Kim, J.H. Seo, D.S. Hwang, A. Masic, D.K. Han, H.J. Cha, Biomacromolecules 15 (2014) 1579—1585.
[78] J.L. Murphy, L. Vollenweider, F. Xu, B.P. Lee, Biomacromolecules 11 (2010) 2976—2984.
[79] M. Mehdizadeh, H. Weng, D. Gyawali, L. Tang, J. Yang, Biomaterials 33 (2012) 7972—7983.
[80] C.E. Brubaker, H. Kissler, L.J. Wang, D.B. Kaufman, P.B. Messersmith, Biomaterials 31 (2010) 420—427.
[81] L. Ninan, R.L. Stroshine, J.J. Wilker, R. Shi, Acta Biomater. 3 (2007) 687—694.
[82] G. Bilic, C. Brubaker, P.B. Messersmith, A.S. Mallik, T.M. Quinn, C. Haller, E. Done, L. Gucciardo, S.M. Zeisberger, R. Zimmermann, J. Deprest, A.H. Zisch, Am. J. Obstet. Gynecol. 202 (2010) 85, e81-85.e89.
[83] A. Kivelio, P. Dekoninck, M. Perrini, C.E. Brubaker, P.B. Messersmith, E. Mazza, J. Deprest, R. Zimmermann, M. Ehrbar, N. Ochsenbein-Koelble, Eur. J. Obstet. Gynecol. Reprod. Biol. 171 (2013) 240—245.
[84] Y. Huang, N.A. Peppas, in: N.A. Peppas, J.Z. Hilt, J.B. Thomas (Eds.), Nanotechnology in Therapeutics: Current Technology and Applications, Horizon Press, Norfolk, UK, 2007, pp. 109—129.
[85] A.M. Lowman, A. Peppas Nicholas, M. Morishita, T. Nagai, Novel Bioadhesive Complexation Networks for Oral Protein Drug Delivery, Tailored Polymeric Materials for Controlled Delivery Systems, American Chemical Society, 1998, pp. 156—164.
[86] A.M. Lowman, N.A. Peppas, J. Biomater. Sci. Polym. Ed. 10 (1999) 999—1009.
[87] P.M. Mannucci, M. Levi, N. Engl. J. Med. 356 (2007) 2301—2311.
[88] E. Haus, Adv. Drug. Deliv. Rev. 59 (2007) 966—984.
[89] L. Yu, J. Gong, C. Zeng, L. Zhang, Mater. Sci. Eng. C: Mater. Biol. Appl. 33 (2013) 3652—3660.
[90] J. Wang, Z. Wang, S. Guo, J. Zhang, Y. Song, X. Dong, X. Wang, J. Yu, Microporous Mesoporous Mater. 146 (2011) 216—222.
[91] D. Johnson, S. Bates, S. Nukalo, A. Staub, A. Hines, T. Leishman, J. Michel, D. Sikes, B. Gegel, J. Burgert, Ann. Med. Surg. 3 (2014) 21—25.
[92] J. McManus, T. Hurtado, A. Pusateri, K.J. Knoop, Prehosp. Emerg. Care: Off. J. Natl. Assoc. EMS Physicians Natl. Assoc. State EMS Dir. 11 (2007) 67—71.
[93] H.B. Alam, Z. Chen, A. Jaskille, R.I. Querol, E. Koustova, R. Inocencio, R. Conran, A. Seufert, N. Ariaban, K. Toruno, P. Rhee, J. Trauma 56 (2004) 974—983.
[94] P. Rhee, C. Brown, M. Martin, A. Salim, D. Plurad, D. Green, L. Chambers, D. Demetriades, G. Velmahos, H. Alam, J. Trauma 64 (2008) 1093—1099.
[95] W.K. Lew, F.A. Weaver, Biologics 2 (2008) 593—599.
[96] M. Sirlak, S. Eryilmaz, L. Yazicioglu, U. Kiziltepe, Z. Eyileten, M.S. Durdu, R. Tasoz, N.T. Eren, A. Aral, B. Kaya, H. Akalin, J. Thorac. Cardiovasc. Surg. 126 (2003) 666—670.
[97] I. Wedmore, J.G. McManus, A.E. Pusateri, J.B. Holcomb, J. Trauma 60 (2006) 655—658.
[98] M.A. Brown, M.R. Daya, J.A. Worley, J. Emerg. Med. 37 (2009) 1—7.
[99] W.L. Hickerson, I. Nur, R. Meidler, Blood Coagul. Fibrinolysis 22 (2011) 19—23.
[100] C. Schonauer, E. Tessitore, G. Barbagallo, V. Albanese, A. Moraci, Eur. Spine. J. 13 (2004) S89—S96.
[101] M.C. Oz, J.F. Rondinone, N.S. Shargill, J. Card. Surg. 18 (2003) 486—493.
[102] M. Gabay, B.A. Boucher, Pharmacotherapy 33 (2013) 935—955.
[103] A. Rickenbacher, S. Breitenstein, M. Lesurtel, A. Frilling, Expert Opin. Biol. Ther. 9 (2009) 897—907.
[104] H.E. Achneck, B. Sileshi, R.M. Jamiolkowski, D.M. Albala, M.L. Shapiro, J.H. Lawson, Ann. Surg. 251 (2010) 217—228 (210.1097/SLA.1090b1013e3181c1093bcca).
[105] A.M. Behrens, M.J. Sikorski, T. Li, Z.J. Wu, B.P. Griffith, P. Kofinas, Acta Biomater. 10 (2014) 701—708.
[106] J.P. Bertram, C.A. Williams, R. Robinson, S.S. Segal, N.T. Flynn, E.B. Lavik, Sci. Transl. Med. 1 (2009) 11ra22.
[107] M. Ravikumar, C.L. Modery, T.L. Wong, A. Sen Gupta, Biomacromolecules 13 (2012) 1495—1502.
[108] Y. Teramura, Y. Okamura, S. Takeoka, H. Tsuchiyama, H. Narumi, M. Kainoh, M. Handa, Y. Ikeda, E. Tsuchida, Biochem. Biophys. Res. Commun. 306 (2003) 256—260.
[109] Y. Okamura, T. Fujie, M. Nogawa, H. Maruyama, M. Handa, Y. Ikeda, S. Takeoka, Transfus. Med. 18 (2008) 158—166.
[110] B.K. Gu, S.J. Park, M.S. Kim, C.M. Kang, J.-I. Kim, C.-H. Kim, Carbohydr. Polym. 97 (2013) 65—73.
[111] Z. Luo, S. Wang, S. Zhang, Biomaterials 32 (2011) 2013—2020.
[112] W.R. Li, X.B. Xie, Q.S. Shi, S.S. Duan, Y.S. Ouyang, Y.B. Chen, BioMetals 24 (2011) 135—141.
[113] R. Kaegi, B. Sinnet, S. Zuleeg, H. Hagendorfer, E. Mueller, R. Vonbank, M. Boller, M. Burkhardt, Environ. Pollut. 158 (2010) 2900—2905.
[114] S. Jadhav, S. Gaikwad, M. Nimse, A. Rajbhoj, J. Clust. Sci. 22 (2011) 121—129.
[115] J.J. Buckley, A.F. Lee, L. Olivi, K. Wilson, Chem. Commun. 34 (2008) 4013—4015.
[116] X.F. Wang, S.L. Zhang, L.Y. Zhu, S.Y. Xie, Z. Dong, Y. Wang, W.Z. Zhou, Vet. J. 191 (2012) 115—120.
[117] A.R. Abbasi, K. Akhbari, A. Morsali, Ultrason. Sonochem. 19 (2012) 846—852.
[118] M. Moritz, M. Geszke-Moritz, Chem. Eng. J. 228 (2013) 596—613.
[119] L. Cheng, M.D. Weir, H.H.K. Xu, J.M. Antonucci, A.M. Kraigsley, N.J. Lin, S. Lin-Gibson, X. Zhou, Dent. Mater. 28 (2012) 561—572.
[120] L. Cheng, M.D. Weir, H.H.K. Xu, A.M. Kraigsley, N.J. Lin, S. Lin-Gibson, X. Zhou, Dent. Mater. 28 (2012) 573—583.
[121] K.R. Raghupathi, R.T. Koodali, A.C. Manna, Langmuir 27 (2011) 4020—4028.
[122] F. Li, P. Wang, M.D. Weir, A.F. Fouad, H.H. Xu, Acta Biomater. (2014).

[123] M.A. Melo, L. Cheng, K. Zhang, M.D. Weir, L.K. Rodrigues, H.H. Xu, Dent. Mater. 29 (2013) 199—210.
[124] Y. Liu, H.I. Kim, Carbohydr. Polym. 89 (2012) 111—116.
[125] S.A. Mousa, R.J. Linhardt, Google Patents, 2012.
[126] A.M. Abdel-Mohsen, R. Hrdina, L. Burgert, R.M. Abdel-Rahman, M. Hasova, D. Smejkalova, M. Kolar, M. Pekar, A.S. Aly, Carbohydr. Polym. 92 (2013) 1177—1187.
[127] J. Wu, Y. Zheng, W. Song, J. Luan, X. Wen, Z. Wu, X. Chen, Q. Wang, S. Guo, Carbohydr. Polym. 102 (2014) 762—771.
[128] Q. Guo, A. Aly, O. Schein, M.M. Trexler, J.H. Elisseeff, Results Pharma Sci. 2 (2012) 66—71.
[129] L.R. Lakshman, K.T. Shalumon, S.V. Nair, R. Jayakumar, S.V. Nair, J. Macromol. Sci. A 47 (2010) 1012—1018.
[130] K. Shalumon, K. Anulekha, S.V. Nair, S. Nair, K. Chennazhi, R. Jayakumar, Int. J. Biol. Macromol. 49 (2011) 247—254.
[131] Z.-x. Cai, X.-m. Mo, K.-h. Zhang, L.-p. Fan, A.-l. Yin, C.-l. He, H.-s. Wang, Int. J. Mol. Sci. 11 (2010) 3529—3539.
[132] D.E. Fullenkamp, J.G. Rivera, Y.K. Gong, K.H. Lau, L. He, R. Varshney, P.B. Messersmith, Biomaterials 33 (2012) 3783—3791.
[133] J.R. Morones-Ramirez, J.A. Winkler, C.S. Spina, J.J. Collins, Sci. Transl. Med. 5 (2013) 190ra181.
[134] E. Dolgin, Nat. Med. 19 (2013) 124—125.
[135] H. Yoon, H.E. Jeong, T.-i. Kim, T.J. Kang, D. Tahk, K. Char, K.Y. Suh, Nano Today 4 (2009) 385—392.
[136] B. Chen, P. Goldberg Oppenheimer, T.A.V. Shean, C.T. Wirth, S. Hofmann, J. Robertson, J. Phys. Chem. C 116 (2012) 20047—20053.
[137] H.E. Jeong, K.Y. Suh, Nano Today 4 (2009) 335—346.
[138] L.F. Boesel, C. Greiner, E. Arzt, A. del Campo, Adv. Mater. 22 (2010) 2125—2137.
[139] N.A. Malvadkar, M.J. Hancock, K. Sekeroglu, W.J. Dressick, M.C. Demirel, Nat. Mater. 9 (2010) 1023—1028.
[140] M.P. Murphy, B. Aksak, M. Sitti, Small 5 (2009) 170—175.
[141] M.P. Murphy, S. Kim, M. Sitti, ACS Appl. Mater. Interfaces 1 (2009) 849—855.
[142] H.E. Jeong, J.-K. Lee, H.N. Kim, S.H. Moon, K.Y. Suh, Proc. Natl. Acad. Sci. USA 106 (2009) 5639—5644.
[143] P. Glass, H. Chung, N.R. Washburn, M. Sitti, Langmuir 25 (2009) 6607—6612.
[144] A. Mahdavi, L. Ferreira, C. Sundback, J.W. Nichol, E.P. Chan, D.J.D. Carter, C.J. Bettinger, S. Patanavanich, L. Chignozha, E. Ben-Joseph, A. Galakatos, H. Pryor, I. Pomerantseva, P.T. Masiakos, W. Faquin, A. Zumbuehl, S. Hong, J. Borenstein, J. Vacanti, R. Langer, J.M. Karp, Proc. Natl. Acad. Sci. USA 105 (2008) 2307—2312.
[145] M.J.N. Pereira, C.A. Sundback, N. Lang, W.K. Cho, I. Pomerantseva, B. Ouyang, S.L. Tao, K. McHugh, O. Mwizerwa, P.K. Vemula, M.C. Mochel, D.J. Carter, J.T. Borenstein, R. Langer, L.S. Ferreira, J.M. Karp, P.T. Masiakos, Adv. Healthc. Mater. 3 (2014) 565—571.
[146] A. Martinelli, G.A. Carru, L. D'Ilario, F. Caprioli, M. Chiaretti, F. Crisante, I. Francolini, A. Piozzi, ACS Appl. Mater. Interfaces 5 (2013) 4340—4349.
[147] K.E. Fischer, B.J. Alemán, S.L. Tao, R. Hugh Daniels, E.M. Li, M.D. Bünger, G. Nagaraj, P. Singh, A. Zettl, T.A. Desai, Nano Lett. 9 (2009) 716—720.
[148] S.Y. Yang, E.D. O'Cearbhaill, G.C. Sisk, K.M. Park, W.K. Cho, M. Villiger, B.E. Bouma, B. Pomahac, J.M. Karp, Nat. Commun. 4 (2013) 1702.
[149] W.K. Cho, J.A. Ankrum, D. Guo, S.A. Chester, S.Y. Yang, A. Kashyap, G.A. Campbell, R.J. Wood, R.K. Rijal, R. Karnik, R. Langer, J.M. Karp, Proc. Natl. Acad. Sci. USA 109 (2012) 21289—21294.
[150] C.-Y. Tsai, C.-C. Chang, J. Mater. Chem. B 1 (2013) 5963—5970.
[151] A.H. Najafabadi, A. Tamayol, N. Annabi, M. Ochoi, P. Mostafalu, M. Akbari, M. Nikkhah, R. Rahimi, M.R. Dokmeci, S. Sonkusale, B. Ziaie, A. Khademhosseini, Adv. Mater. 26 (2014) 5823—5830.
[152] S.-W. Hwang, H. Tao, D.-H. Kim, H. Cheng, J.-K. Song, E. Rill, M.A. Brenckle, B. Panilaitis, S.M. Won, Y.-S. Kim, Y.M. Song, K.J. Yu, A. Ameen, R. Li, Y. Su, M. Yang, D.L. Kaplan, M.R. Zakin, M.J. Slepian, Y. Huang, F.G. Omenetto, J.A. Rogers, Science 337 (2012) 1640—1644.